Monsoonal rainfall initiates autochthonous alteration of dissolved organic matter composition in Indian groundwaters

George J.L. Wilson [a], David A. Aind [b], Abhijit Mukherjee [b,c], David A. Polya [a],
Daren C. Gooddy [d,1,2], Laura A. Richards [a,*]

[a] Department of Earth and Environmental Sciences and Williamson Research Centre for Molecular Environmental Science, The University of Manchester, Williamson Building, Oxford Road, Manchester, M13 9PL, United Kingdom
[b] Department of Geology & Geophysics, Indian Institute of Technology Kharagpur, Kharagpur, 721302, India
[c] School of Environmental Sciences and Engineering, Indian Institute of Technology Kharagpur, Kharagpur, 721302, India
[d] British Geological Survey, Maclean Building, Wallingford, Oxfordshire, OX10 8BB, United Kingdom

ARTICLE INFO

ABSTRACT

Groundwater contamination is a considerable threat to public health in many regions of the world. Strong seasonal variation in monsoon-affected regions can have significant effects on groundwater quality, yet these variations are not fully understood. Using excitation-emission matrix (EEM) fluorescent spectroscopy, we explore the seasonal dynamics of dissolved organic matter (DOM) composition along a transect in West Bengal, India. Groundwater, river water and ponds were sampled ($n = 59$) on a weekly/fortnightly basis, from the onset of monsoon to late-July, to gain an understanding of DOM temporal dynamics in aquifers at a critical point in seasonal hydrological conditions. Several fluorescent DOM (fDOM) components and indices were used to infer the source and nature of DOM. Although dissolved organic carbon (DOC) remained consistent throughout the sample timeframe, precipitation-associated spikes in fluorescence index (FI), specific ultraviolet absorbance (SUVA$_{254}$) and redox potential (*Eh*) likely point towards rainfall-induced increase of autochthonous DOM and the increase of microbial metabolic activity in response to oxygenated recharge. We suggest that observed fluctuations in organics were associated with concomitant changes in redox- and solubility-controlled elements (*e.g.* Fe and Mg), thus having wider implications on groundwater geochemistry and particularly the mobility of redox- and organic-sensitive solutes.

1. Introduction

Deterioration of groundwater quality presents a significant threat to global water security (Lapworth et al., 2022; McDonough et al., 2020). Compounds that comprise dissolved organic matter (DOM) play a fundamental role in aqueous systems by providing a substrate for microbially mediated processes (Aftabtalab et al., 2022; Postma et al., 2007; Rowland et al., 2007; Wallis et al., 2020) and altering water chemistry (Brailsford et al., 2017; Qualls and Richardson, 2003). Of particular relevance to human health, DOM can alter the mobility of organic pollutants (Evans et al., 2019) and trace metal(loid)s (Aftabtalab et al., 2022; Benedetti et al., 1996; Farooq et al., 2010; Islam et al., 2004; Kwak et al., 2024; Lawson et al., 2016; Mladenov et al., 2010; Postma et al., 2007; Ren et al., 2015; Richards et al., 2019a; Rowland et al., 2007; Schaefer et al., 2016; Wallis et al., 2020). Therefore, exploring the behaviour of DOM in aqueous systems proves to be an important step in understanding the quality of groundwater resources.

Understanding DOM in the environment is impeded due to its inherent chemical complexity and non-specific nature. Traditionally, DOM has been quantified by bulk methods, *e.g.* total organic carbon (TOC) or biological oxygen demand (BOD), and further characterised by spectrometry and/or chromatography, *e.g.* liquid chromatography-mass spectrometry (LC-MS), Fourier transform infrared (FTIR) spectroscopy (Berthomieu and Hienerwadel, 2009) or nuclear magnetic resonance (NMR) spectroscopy (Dittmar and Paeng, 2009; Matilainen et al., 2011), but these methods are resource-intensive (Leenheer and Croué, 2003).

---

* Corresponding author.
 E-mail address: laura.richards@manchester.ac.uk (L.A. Richards).
[1] (Current) UKCEH, Maclean Building, Wallingford, Oxfordshire, OX10 8BB, United Kingdom.
[2] (Current) Lancaster Environment Centre, Lancaster University, Lancaster, LA1 4YQ, United Kingdom.

Recent analytical advance based on the fluorescent properties of DOM under UV light, namely fluorescence spectroscopy, has proven to be an insightful, comparatively inexpensive and rapid method for DOM characterisation (Kulkarni et al., 2017; McKnight et al., 2001; Mladenov et al., 2010; Murphy et al., 2013; Niloy et al., 2021; Osburn et al., 2017; Sgroi et al., 2017; Stedmon and Markager, 2005; Wünsch et al., 2019) and also an auspicious *in-situ* method of groundwater quality monitoring of DOM (Sorensen et al., 2020, 2021). Fluorescent DOM (fDOM) can be measured by recording the intensity of emission wavelength as a function of excitation; the resultant three-dimensional excitation-emission matrix (EEM) can be used to characterise DOM source and nature (McKnight et al., 2001; Stedmon and Markager, 2005; Wünsch et al., 2019). Importantly, this characterisation method can distinguish between autochthonous (produced *in-situ* by microorganisms and aquatic macrophytes) and allochthonous (from degraded terrestrial material) DOM, for example (McKnight et al., 2001; Pagano et al., 2014).

The influence of seasonality on aqueous systems is well documented (Farooq et al., 2010; Jameel et al., 2023; Kulkarni et al., 2018; Luzius et al., 2018; Yang et al., 2020). However, while temporal changes in DOM composition in rivers have been extensively studied (Niloy et al., 2021; Singh et al., 2020; Yamashita et al., 2011), groundwater has received comparatively less attention. Notably, certain studies have reported the prevalence of humic-derived components in groundwater following the onset of monsoon, compared to the non-monsoon season (Chen et al., 2018; Kulkarni et al., 2018; Wilson et al., 2023; Yang et al., 2020). Evidence suggests that DOM alteration may be induced after precipitation events, as surface-derived substrates required for primary productivity are introduced into aquifers (Howard et al., 2003; Kuzyakov, 2010; Sorensen et al., 2018b, 2021; Ward et al., 2021; Worrall and Burt, 2004; Worthington and Smart, 2017). This effect may be particularly pronounced in aquifers where there is substantial flow rate and surface-derived bacteria can travel hundreds of meters from source before attenuation takes place (Sorensen et al., 2018b; Worthington and Smart, 2017). Indeed, surface-derived ingress to groundwater has been demonstrated to be highly dependent on lithology (*e.g.* clay-versus sand-dominant; Richards et al., 2019b, 2017; Uhlemann et al., 2017) as well as borehole-induced bypass flow (Banks et al., 2021; Ercumen et al., 2017).

Deteriorating water quality presents future challenges for water supplies in India, particularly in the drought-prone eastern state of West Bengal (Bhunia et al., 2020; CGWB, 2023; Chatterjee, 2024; Dangar et al., 2021; Jain et al., 2021; Jana et al., 2009; John et al., 2018; Rodell et al., 2009; Sarkar and Ray, 2015). Here, increasing frequency of drought calls for the sustainable management of water resources for drinking and irrigation purpose (Bhunia et al., 2020; Roy et al., 2023). In West Bengal, monsoon-attributed variations in geochemistry were reported (Farooq et al., 2011; Kulkarni et al., 2018; Majumder et al., 2016; Mohanta and Goel, 2014). However, these studies have been limited in sampling frequency, making it difficult to comprehend groundwater DOM variability during periods of distinct hydrological change, such as the onset of the monsoon season.

In this study, we examine DOM (bulk and fDOM) and inorganic geochemistry to quantify and elucidate temporal changes in groundwater DOM composition in a transect of groundwater and surface water sites in West Midnapore district, West Bengal, covering a period of rapid increase in well hydraulic head (i.e., at the onset of monsoon; Jameel et al., 2023). We aim to test the hypothesis that at the onset of monsoon there will be precipitation-associated compositional changes in DOM and geochemistry and that this is influenced by the underlying lithology.

2. Methodology

2.1. Site description

Groundwater and surface water samples were collected in the water-stressed West Midnapore district along a 40 km NE-SW-orientated transect (Fig. 1b). The transect intersects the Kansabati and Subarnarekha rivers in the north and south, respectively, and lies parallel to the Medinipur-Farraka (MFF) basement fault (Singh et al., 1998). The sub-surface between Kharagpur and Nayagram, has previously been characterized by vertical electrical sounding (Fig. 1a; Panda et al., 2018). Younger alluvial sediments prevail at 0–15 m depth in the southern part of the transect, such that the southern part of the transect has been earmarked for use as an artificial recharge site (Panda et al., 2018), whilst laterites at shallow depth create an impervious layer above older platform sediments around Kharagpur (Chowdhury et al., 2010; Ghosh et al., 2015; Panda et al., 2018). Below the alluvium, an unconsolidated to semi-unconsolidated layer of sand and gravel exists (Chowdhury et al., 2010). The net groundwater flow direction in West Midnapore is NW–SE (CGWB, 2022). West Midnapore experiences a humid sub-tropic climate with an average rainfall of 1527 mm (1127 mm in monsoon and 400 mm during non-monsoon; CGWB, 2022). Daily rainfall data was obtained from Mohanpur station, West Bengal (30–50 km from the transect) from the Indian Meteorological Department (IMD) Grid Model dataset, for the duration of the sampling period (Pai et al., 2014).

2.2. Groundwater and surface water sampling

Samples ($n = 59$) were taken from private and government pumps ($n = 10$; 14–91 m depth), rivers ($n = 2$) and surface ponds ($n = 3$) at the onset of the monsoon season (18 June to 27 July, 2022) at a weekly or fortnightly interval (Fig. 1). Sampling of sites depended on the compliance of landowners and the accessibility of the water source. Samples for i) total organic carbon (TOC), ii) EEM, iii) stable water isotopes and iv) anions/cations were filtered with Sartorius regenerated cellulose membrane filters (0.45 μm) and stored in amber glass (organics), clear glass (anions/cations and isotopes) bottles at 4 °C until analysis. Chemical preservation was not undertaken due to dangerous goods restrictions on the transportation of nitric acid. All bottles were acid-washed (10% HNO_3) and furnaced before use. Measurements of pH and oxidation-reduction potential (ORP) were made with HI98128 and HI98120 m (Hanna Instruments, UK), calibrated daily with a 2-point calibration at pH 7 and 10 and HI 7021 ORP solution, respectively.

2.3. DOC measurements

Bulk DOC was quantified using a Shimadzu® Total Organic Carbon Analyser (TOC-VCPN) with an ASI-V autosampler at the Manchester Analytical Geochemical Unit (MAGU) laboratory (The University of Manchester). Dissolved organic carbon (DOC) as non-purgeable organic carbon (NPOC), was quantified using the 680 °C combustion catalytic oxidation method.

To characterise the source and nature of DOM, fluorescence spectroscopy measurements were made using a Varian Cary Eclipse fluorescence spectrophotometer, at the British Geological Survey (Wallingford, UK) during September 2022. Samples were scanned at an excitation wavelength from 200 to 400 nm with 5 nm increment and an emission wavelength of 250–500 nm with 2 nm increment, in a quartz cuvette with 1-cm path length. The EEM data was reported following blank subtraction and removal of Rayleigh scatter lines. The reported intensity was normalised to Raman Units (RU) by dividing by the Raman peak of ultrapure water (Murphy, 2011). Ultraviolet absorbance at 254 nm (Abs_{254}) was measured using a Varian UV–vis spectrophotometer with the same sample aliquot and cuvette used for fluorescence analysis. ASTM type I reagent grade ultrapure water was used for blanks and to clean the glass cuvette between samples. Data was absorbance-corrected to account for inner filter effect (IFE) using a method from Lakowicz (1994).

The resultant excitation-emission matrix (EEM) was analysed by quantifying specific wavelength regions: i) fulvic acid-like (FA-like), ii) tryptophan-like (Tryp-like), iii) Tryp:FA – the ratio of Tryp-like to FA-
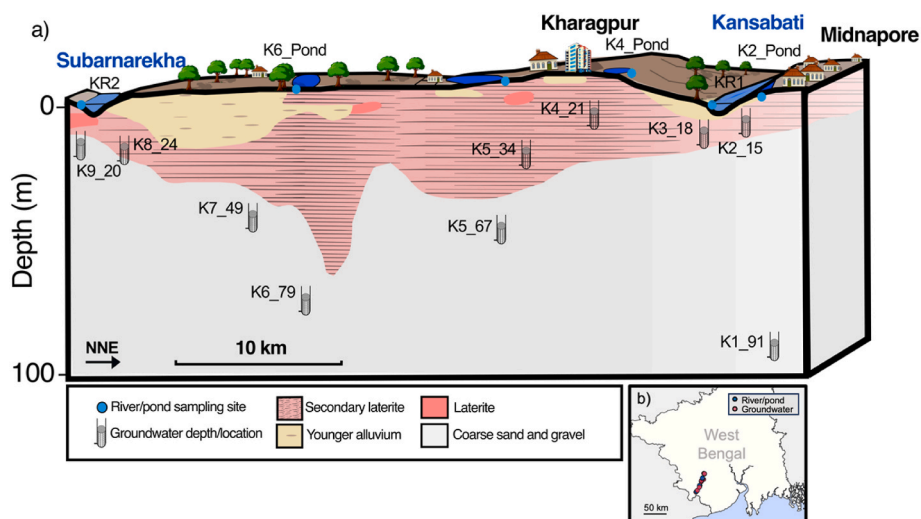
Fig. 1. Groundwater (14–91 m depth) and surface water sampling sites between Nayagram and Midnapore a) overlain on the transect geology as a block diagram and b) in the state of West Bengal, India. Samples were taken from private and government pumps ($n = 10$; borehole symbol), rivers ($n = 2$; blue dots) and surface ponds ($n = 3$; blue dots) at the onset of the monsoon to late July. The subsurface was extrapolated from resistivity and geological observation reported in Panda et al. (2018) and Chowdhury et al. (2010). The sites were named 'K(site number)_(reported depth in m; R1 = Kansabati River; R2 = Subarnarekha River)'. (For interpretation of the references to colour in this figure legend, the reader is referred to the Web version of this article.)

like fluorescence, which differentiates between labile and recalcitrant sources of DOM (Baker, 2002; Sorensen et al., 2018a), iv) fluorescence index (FI) – used to distinguish between microbial and terrestrial DOM (Cory and McKnight, 2005; McKnight et al., 2001), v) the beta to alpha (β:α) ratio, indicating the degree of DOM 'freshness' (Kulkarni et al., 2017; Parlanti et al., 2000), vi) humification index (HIX) to determine the degree of humification (Ohno, 2002) and vii) specific ultraviolet absorbance at 254 nm (SUVA$_{254}$) as an indicator of DOM aromaticity (Weishaar et al., 2003). Data processing and index calculations were performed using R (R Core Team, 2023) according to Lapworth and Kinniburgh (2009).

2.4. Quantification of anions and cations

Quantification of anions (F$^-$, Cl$^-$, Br$^-$, NO$_2^-$, NO$_3^-$, SO$_4^{2-}$ and PO$_4$) was carried out using ion chromatography (IC; Dionex ICS5000 Ion Chromatograph and Dionex IonPac AS18 columns) at MAGU. Selected major elements (Ca, Fe, K, Mg, Na, S and Si) were quantified by inductively coupled plasma optical emission spectrometry (ICP-OES, PerkinElmer Optima 5300 dual view) at MAGU. Sr was quantified using inductively coupled plasma mass spectrometry (ICP-MS; Agilent 7500cx) at MAGU. Samples for ICP-OES/MS were acidified to 2 % HNO$_3$ (Aristar®, VWR Chemicals BDH®, UK) before analysis to ensure analytes were fully dissolved in solution at the time of analysis. Cation data, including calculations of the standard deviation were instrument-corrected using a weighted calibration regression according to Miller and Miller (2010). Alkalinity as HCO$_3^-$ was estimated solely from the difference between the total cationic (Σ^+) and anionic (Σ^-) charge ([HCO$_3^-$] = $\Sigma^+ - \Sigma^-$; Boyd et al., 2011). Multi-element Certified Reference Materials (CRMs; LGC6020, LGC6026, LGC6027 and VHG-ICM1-500, LGC Standards, UK and QC1364, Sigma Aldrich, USA) were used to verify the quality of the data.

2.5. Isotopic analysis

Stable isotopes (O and H) for all sites ($n = 15$) were quantified using cavity ring-down spectroscopy (CRDS; Picarro L2120-i). Due to resource constraints, only one timepoint at the end of July was sub-sampled for stable isotopes to identify possible mixing processes between surface water and groundwater. Samples were stored in 1.5 mL airtight glass vials and were analysed on the same day of sampling at the School of Environmental Science and Engineering, Indian Institute of Technology Kharagpur (IITKGP). Stable isotopic fractions of hydrogen are denoted by δ^{18}O (^{18}O/^{16}O) and δ^{2}H (^{2}H/^{1}H) expressed as parts per thousand (‰) depletions relative to the Vienna Standard Mean Oceanic Water (VSMOW; Gonfiantini, 1978). Analytical errors of the isotope measurements were reported to 1-σ.

3. Results

3.1. Data quality

A number of measurements were made to assess the quality of the data and the variation between sub-samples. The mean analytical repeat ($n = 7$) error for anions quantified by IC (F$^-$, Cl$^-$, Br$^-$, NO$_2^-$, NO$_3^-$, SO$_4^{2-}$ and PO$_4$) was 1.6 %, 1.1 %, 4.0 %, 10.6 %, 5.7 %, 2.7 % and 1.5 %, respectively, whilst the sampling repeat ($n = 3$) error was 1.9 %, 0.7 %, 2.2 %, 25.0 %, 1.4 %, 1.5 % and 10.7 %. The mean CRM (QC1364, LGC6020 and ICM1-500) bias for listed anions was 3.6 %, 0.8 %, 1.3 %, 7.1 %, 4.4 %, 1.9 % and 11.5 %, respectively.

For cations measured by ICP-OES (Ca, Fe, K, Mg, Na, S and Si), the analytical repeat ($n = 7$) error was 1.0 %, 33.1 %, 9.5 %, 1.2 %, 5.7 %, 3.8 % and 4.5 %, respectively, whilst the sampling repeat ($n = 3$) error was 2.6 %, 145.0 %, 21.9 %, 1.1 %, 0.9 %, 5.3 % and 1.6 %, respectively. We note that the repeated samples for Fe were all below 0.1 mg/L, which may explain the relatively large sampling and analytical errors for Fe. The average CRM (LGC6026 and LGC6027) bias for Ca, Fe, K, Mg and Na was 0.2 %, 3.6 %, 39.9 %, 2.4 % and 27.7 %, respectively. A high observed CRM bias for K (71.8 %) for LGC6027 was likely because the expected concentration of the standard (0.63 mg/L) was close to the analytical detection limit.

The analytical repeat ($n = 7$) and sampling repeat ($n = 3$) error for NPOC was 17.6 % and 52.5 %, respectively. The analytical repeat ($n = 7$) error of fDOM measurements (FA-like, Tryp-like, FI and β:α) was 47.8 %, 85.0 %, 33.5 % and 102.9 %, respectively, whilst the sampling repeat ($n = 2$) error was 19.1 %, 63.5 %, 122.0 % and 25.3 %, respectively. The repetition of samples with low NPOC (<1 mg/L) and calculations of indices at regions of very low fluorescence intensity likely gave rise to substantial reported sampling and analytical errors.

The reported accuracy of the pH and ORP meters was ±0.01 and ±

0.2 mV, respectively, according to the manufacturer. The repeat measurement error in the field was typically ±0.1 for pH and ±15 mV for ORP.

3.2. Temporal changes in groundwater DOM and geochemistry

A time series sampling approach was used to identify potential rainfall-induced changes in (f)DOM and selected geochemical parameters at the onset of monsoon. There were three major rainfall events of increasing intensity during the sampling period (Fig. 2c). Large spikes in redox potential (*Eh*) were observed in K5_67 and K5_34 around the second rainfall period (Fig. 2a) and corresponded to a spike in NO_2^- in K5_34 (Fig. S1c) that may indicate partial nitrification of NH_4^+. These observations point towards the presence of rapid recharge of more oxygenated water around the K5 sampling area. *Eh* generally decreased throughout the 1.5-month time series, potentially indicating oxygen consumption during the oxidation of DOM.

Bulk DOC remained consistent in groundwater and pond samples during the timeframe, except K4_Pond which decreased notably from 8.3 to 5.5 mg/L throughout the time series. Kansabati (KR1) and Subarnarekha (KR2) river samples exhibited a large increase in fulvic-like DOC in the latter half of the time series (Fig. 2b–j; orange lines), plausibly as mobilisation of upstream sediments increased in response to increased river stage. Groundwater at K5_67 also exhibited a 4-fold increase in DOC on 27 July. The β:α was consistently ~1 for surface water

sites, although there were substantial spikes in β:α in groundwater samples K5_34 and K4_21 (Fig. 2h). In fact, site K4_21 displayed increases in β:α, FI and Tryp:FA markers following rainfall, noting very low apparent resistivity reported around this site (Panda et al., 2018). Site K5_34, K6_79, K2_15, K8_24, K5_67 also observed an increase in FI which seemed to track major rainfall events, suggesting a precipitation-induced increase in autochthonously produced DOM (McKnight et al., 2001). Similarly, increased FI was also observed from pre-to post-monsoon groundwater in Bihar, northern India (Wilson et al., 2023).

In groundwater, FA-like DOM displayed consistency in all sites throughout the time series, though a spike was observed in site K5_34 around the second and third rainfall events. A spike in FA- and Tryp-like fDOM in site K5_67 in July in conjunction with a spike in *Eh*, following a large rainfall event on 02 July, could indicate the ingression of allochthonous DOM and surface-derived substrates into groundwater (Figure S1e, f and Fig. 2a; Chen et al., 2022; Luzius et al., 2018). Site K5_67 also exhibited a 50-fold increase in $SUVA_{254}$ on 05 July from 28 June, suggesting that the reactivity of DOM increased following rainfall (Fig. 2g; Weishaar et al., 2003). Whilst plausible, both FA-like and tryptophan-like may be produced by autochthonous microbial processing (Fox et al., 2017). A spike in Tryp-like and β:α in K5_34 during a dry period (Figure S1f and Fig. 2h) was not seen elsewhere in the data.

Piper classification revealed a predominant Ca–HCO_3^- water type (Fig. 3), which is consistent with pre-monsoon/monsoon/post-monsoon
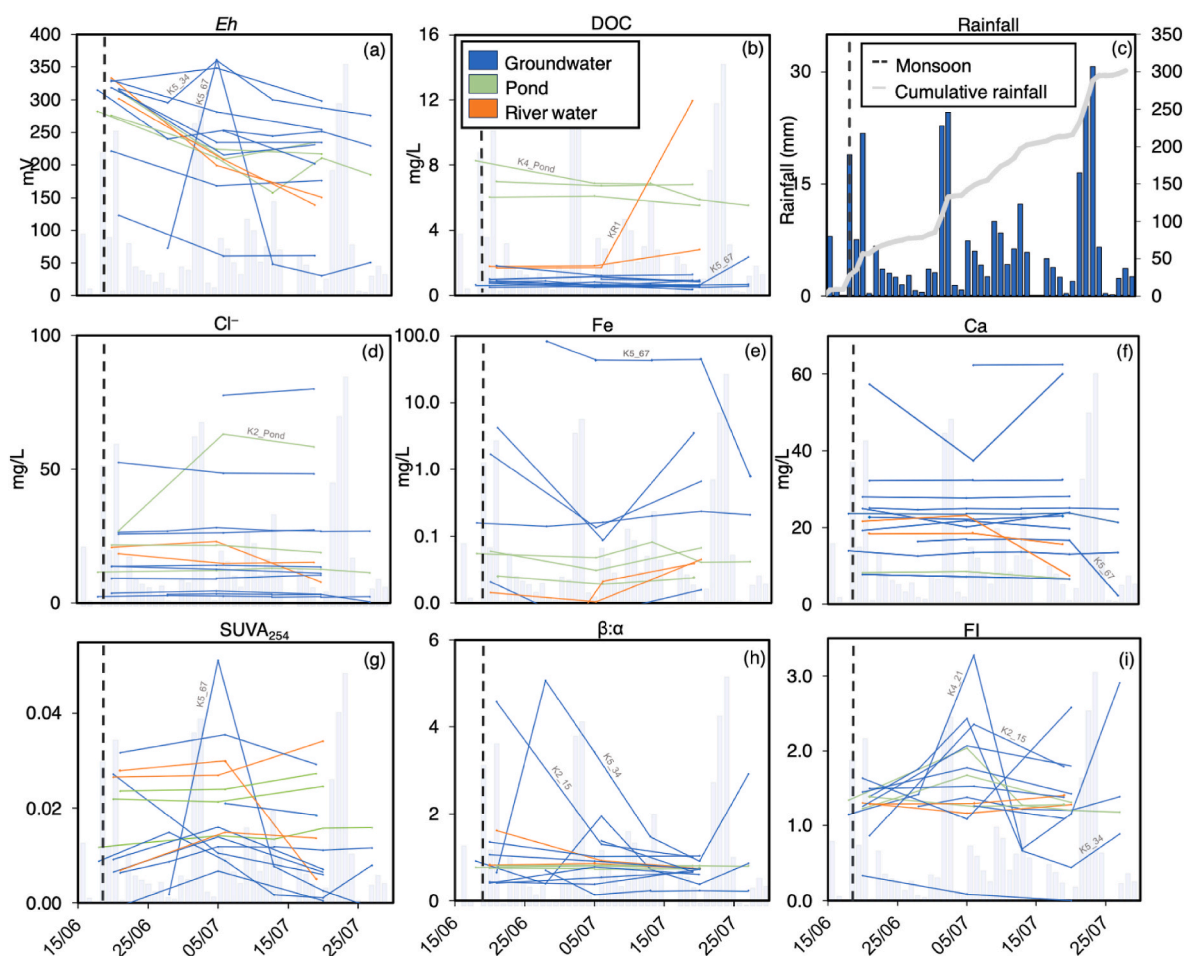

Fig. 2. Time series plots of groundwater characteristics at the onset of monsoon revealed consistency in chloride and NPOC, though *Eh*, total iron and fluorescence DOM markers revealed systematic changes in the sampled period. Fluorescence measurements were normalised to Raman Units (RU) according to Murphy (2011). Rainfall is displayed in **c** as cumulative rainfall (grey line) and as daily rainfall (blue bars) at Mohanpur, West Bengal from the Indian Meteorological Department (IMD) Grid dataset (Pai et al., 2014). Daily rainfall is superimposed on all plots. (For interpretation of the references to colour in this figure legend, the reader is referred to the Web version of this article.)
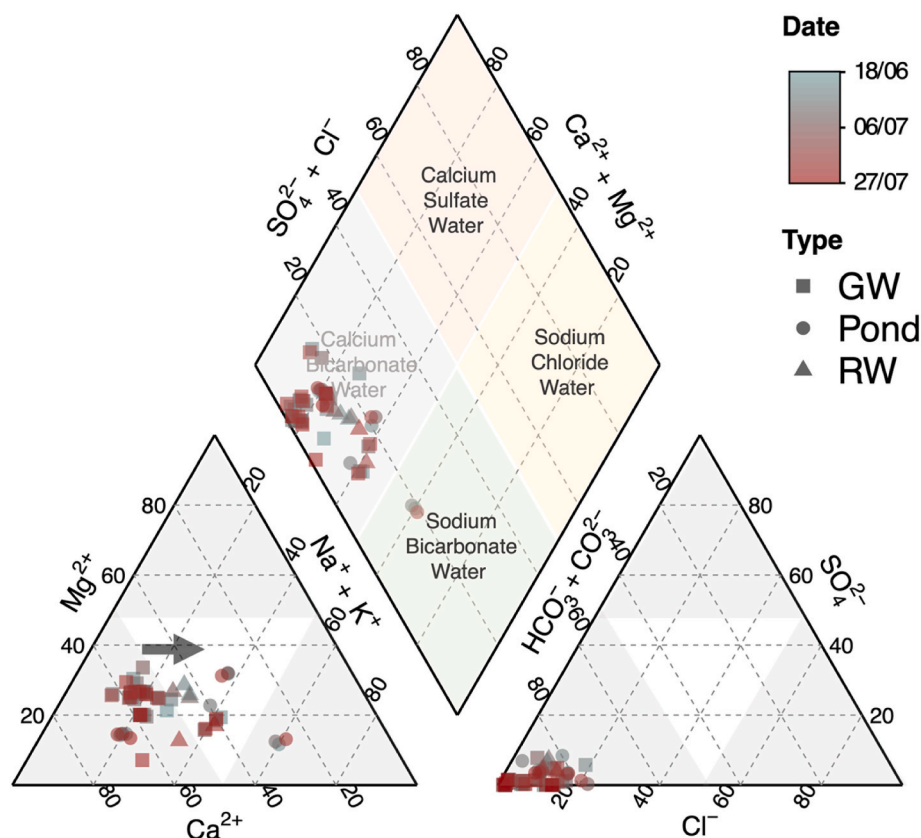
Fig. 3. Piper diagram of groundwater (GW), river water (RW) and ponds in West Bengal reveals consistency in major geochemistry of Ca–HCO$_3^-$ type albeit a reduction in Ca proportion in some sites at the onset of monsoon (grey arrow; Piper, 1944). Major anions and cation were measured using ion chromatography (IC) and inductively coupled plasma optical emission spectrometry (ICP-OES), respectively. HCO$_3^-$ and CO$_3^{2-}$ as alkalinity was estimated from the discrepancy in the charge balance of major positive and negative ions.

groundwater in the Murshidabad District, West Bengal (Farooq et al., 2011; Piper, 1944). Though major geochemistry was reasonably constant across the sampling time period, a large decrease in Fe was observed in site K5_67, potentially as a result of oxidation from soluble Fe(II) into insoluble Fe(III) oxide. Interestingly, semiquinone-like moieties, measured by FI (Cory and McKnight, 2005), have been shown to drive fluctuations in redox-sensitive elements such as iron (Fig. 2e; Jiang et al., 2015), though a time lag between increase in FI and decrease in total Fe remains unexplained. Chloride, as a conservative tracer for dilution/evaporation was reasonably consistent in all sites throughout the time series, except for K2_Pond which exhibited a two-fold increase in chloride from June–July (Fig. 2d).

Dissolved organics have been shown to be interconnected with calcite-water reactions (Kerr et al., 2021; Kim and Lee, 2009). A reduction in proportion of Ca compared to Mg in sites such as K5_67 (Fig. 3) plausibly suggest precipitation of Ca (Pracný et al., 2019; Sinclair et al., 2012). Changes in ln(Mg/Ca) compared to ln(Sr/Ca) in K2_15 resemble a gradient of 0.85 (Fig. 4), which Sinclair et al. (2012) have suggested to indicate prior calcite precipitation (PCP). This localised observation could arise from an increase in alkalinity and consequential increase to calcite saturation states (Sulpis et al., 2022). Although inferred alkalinity was relatively constant in most sites, a few sites exhibited an increase (Fig. 3), which could plausibly expedite carbonate precipitation. Importantly, DOM may fundamentally contribute to alkalinity as organic alkalinity (Kerr et al., 2021) and through oxidation of organic compounds into carbon dioxide. Thus, a plausible explanation is that the degradation or processing of DOM contributes to changes to solubility-controlled dissolved species.
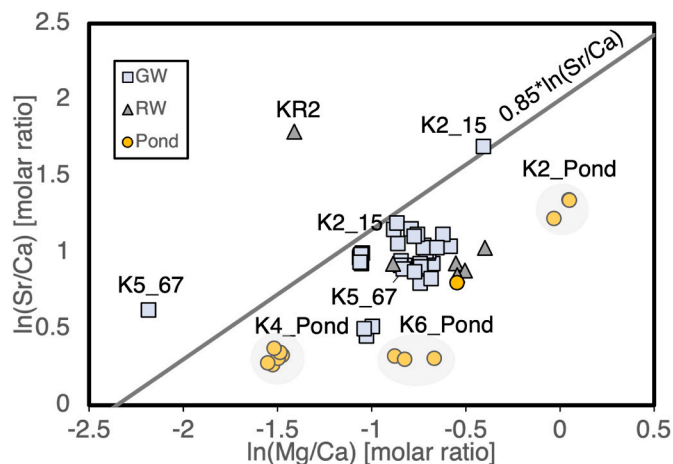

Fig. 4. Ratios of ln(Mg/Ca) and ln(Sr/Ca) showed that incongruent dissolution and prior calcite precipitation could have occurred in K2_15 during the sampling time series. The black line plots ln(Mg/Ca) = 0.85*ln(Sr/Ca) from (Sinclair et al., 2012). Samples were taken from private and government pumps (n = 10; squares), rivers (n = 2; triangles) and surface ponds (n = 3; circles) at the onset of the monsoon to late July.

3.3. Temporal changes in geochemistry as a function of depth and geological setting

Geochemistry was characterised as a function of reported depth to understand hydrogeology-associated temporal changes across the

sampling timeframe. Temporal changes in groundwater DOC and FI did not seem to be associated with depth (Fig. 5a–c). On the other hand, decreases in groundwater *Eh*, Tryp-like and FA-like fDOM over the time series were more pronounced in shallow sites associated with laterites (Fig. 5b, d, e), compared to groundwater derived from predominantly sand and gravel lithology (Panda et al., 2018). This observation could suggest a rapid oxidation of DOM at shallower depths during the sampling period.

3.4. Stable water isotopes

Analysis of stable isotopes was conducted at the end of the sampling period to disentangle possible mixing processes between surface water and groundwater (Fig. 6). Pond samples (n = 3) exhibited elevated $\delta^{18}O$ (mean = 1.9 ± 0.2 ‰) and δ^2H (mean = −11.3 ± 0.5 ‰) compared to groundwater and river water sites, suggesting water from sampled ponds has undergone a relatively large degree of evaporative enrichment. Sites K5_67, K6_79 and K9_20 plot closest to the GMWL and LMWL, suggesting these samples could be comprised of a larger proportion of recent rainfall, compared to water which has undergone evaporative enrichment (*e.g.* soils and ponds). Interestingly, dry season groundwater from the Murshidabad district, West Bengal, exhibited a much more precipitation-dominated signature than samples in this study (Datta et al., 2011). This could indicate that precipitation-derived infiltration in West Midnapore is not pervasive and may suggest that rapid recharge occurs on a localised (*i.e.* borehole) scale and that the phenomena are not aquifer-wide.

A distinct similarity between river (KR1 and KR2; mean = −1.9 ± 0.2 ‰ $\delta^{18}O$ and −23.5 ± 0.4 ‰ δ^2H) and near-bank groundwater sites adjacent to the Kansabati (K3_18 and K2_15; mean = −2.0 ± 0.2 ‰ $\delta^{18}O$ and −22.7 ± 0.45 ‰) may suggest a strong baseflow component to the Kansabati and Subarnarekha rivers and/or a monsoon reversal in hydraulic head causing water to flow from the Kansabati to near-bank shallow groundwater, potentially expedited by groundwater abstraction from Midnapore and Kharagpur (Fig. 1; Benner et al., 2008; Lu et al., 2022; Richards et al., 2017).

4. Discussion

This study investigated the compositional changes in groundwater DOM and geochemistry at the onset of monsoon. Sudden availability of surface-derived substrates has previously been thought to increase the
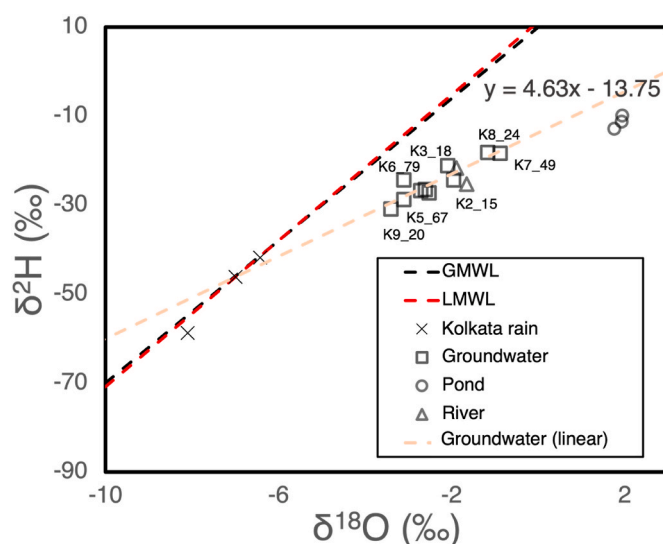

Fig. 6. $\delta^{18}O$ ($^{18}O/^{16}O$) and δ^2H ($^2H/^1H$) cross-plot of groundwater, pond and river water sampled from the studied transect in West Midnapore (West Bengal) in late July 2022. Isotopic signatures of $\delta^{18}O$ and δ^2H are expressed as parts per thousand (‰) depletion relative to the Vienna Standard Mean Oceanic Water (VSMOW; Gonfiantini, 1978). LMWL = Local Meteoric Water Line (red dashed line) from Bengal basin precipitation (Jameel et al., 2023). GMWL = Global Meteoric Water Line (black dashed line; δ^2H = 8 *$\delta^{18}O$ + 10; Craig, 1961). Three rain samples (black crosses) were from monsoon season (2022) in Kolkata (IAEA/WMO, 2017). (For interpretation of the references to colour in this figure legend, the reader is referred to the Web version of this article.)

productivity of microbial communities on a scale of days to weeks (Hofmann et al., 2020; Kuzyakov, 2010), though limited evidence has supported this claim in the literature (Hofmann et al., 2020). It has been suggested that the addition of reactive carbon may increase primary production in aquifers by increasing microbial metabolism of sedimentary organic carbon (SOC; Bianchi, 2011; Fang et al., 2023; Fontaine et al., 2007; Schmidt et al., 2011). Whilst groundwater DOC remained constant across the time series in the present study, fluorescence markers revealed compositional changes at the onset of monsoon.

The observed association between rainfall, spikes in fDOM and *Eh* suggest that monsoonal recharge oxygenates the aquifer and promotes microbial metabolism. This likely drives the production of semiquinone-
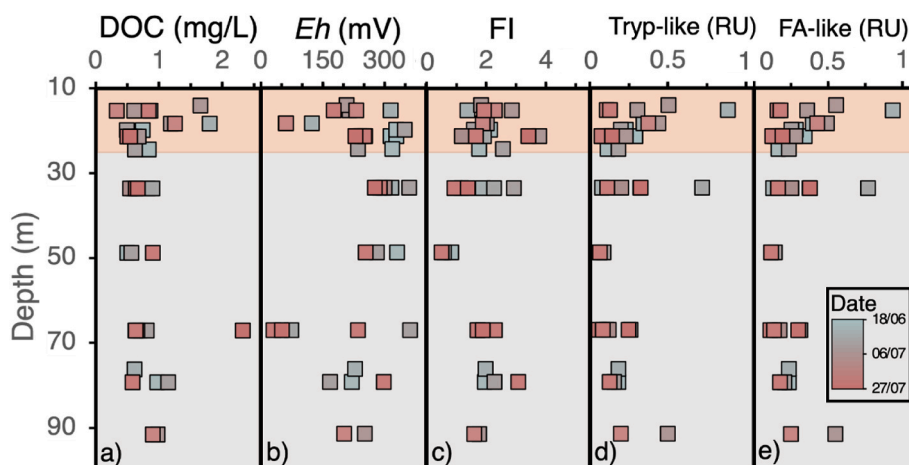

Fig. 5. Temporal shifts in West Bengal groundwater in organics and geochemical parameters: a) dissolved organic carbon (DOC) as non-purgeable organic carbon (NPOC), b) redox potential (*Eh*), c) Fluorescence Index (FI; McKnight et al., 2001), d) Tryptophan-like fluorescent DOM (Tryp-like) and e) Fulvic acid-like fluorescent DOM (FA-like), as a function of reported depth. Fluorescence measaurements were normalised to Raman Units (RU) according to Murphy (2011). The pink shaded region represents an approximated depth of lateritic-dominated geology whilst the grey shaded region represents coarse sand and gravel in the sample transect (Panda et al., 2018). (For interpretation of the references to colour in this figure legend, the reader is referred to the Web version of this article.)

like fluorescent components, associated with increased FI (Cory and McKnight, 2005), plausibly through the activation of oxygen-dependent enzymes (Worrall and Burt, 2004, 2007). A sustained ~50 mm rainfall event between 02 and 03 July appeared to influence many parameters (*Eh*, FI, SUVA$_{254}$, NO_2^- and FA-like DOM), but only in specific groundwater sites and this can plausibly be explained by hydrogeology.

In West Midnapore, groundwater vulnerability to bacterial contamination is likely reduced by unconsolidated aquifers, which facilitate sorption and filtration via intergranular flowpaths (Chowdhury et al., 2010; Panda et al., 2018; Worthington and Smart, 2017). In contrast, consolidated laterite rock around Kharagpur may exhibit more macropore flow, as this geology may be more susceptible to cracking, compared to alluvium (Groeneveld et al., 2020; Liu and She, 2020). Indeed, sites overlying laterites, particularly K5, expressed fluctuations in *Eh*, Fe, NO_2^-, FA-like and Tryp-like fDOM and DOC (Fig. 2; Fig. S1) along with a more precipitation-derived isotopic signature (Fig. 6). Although the ingress of meteoric water may be affected by the depositional environment (McArthur et al., 2010; Mukherjee, 2022; Neidhardt et al., 2013), the geophysical study did not identify paleochannels around Kharagpur (Panda et al., 2018). Based on this rationale, the physical characteristics of the wells or fractures in the rocks are perhaps more likely to contribute to rapid surface-derived ingress into groundwater, as opposed to pervasive recharge through lateritic cover (Banks et al., 2021; Ercumen et al., 2017; Hynds et al., 2012). Although this study did not assess the borehole annulus (Takavada et al., 2022), ineffective borehole sealing could provide a potential and substantial mechanism for microbial contamination to bypass intergranular filtration (Klose et al., 2021; Worthington and Smart, 2017). Additionally, pumping-induced shear stress on sediments may contribute to biofilm sloughing and the release of SOC (Graham et al., 2015). Indeed, Midnapore and Kharagpur are most likely to be most affected by intensive pumping regimes (CGWB, 2023).

The formation of insoluble Fe(III) oxides from microbially induced laterization may be expedited by aquifer re-oxygenation (Ghosh et al., 2015; Li et al., 2017), which was substantiated by rainfall-associated spikes in *Eh* and evidence from stable water isotopes (Fig. 6). The possible production of microbially derived semiquinone-like DOM, as indicated by increases in FI (Cory and McKnight, 2005), plausibly alters the redox state of Fe (Jiang et al., 2015). However, no evidence suggested that total Fe was a major control on the system leading to the production of autochthonous DOM. Whilst some changes in geochemistry were observed (*e.g.* Ca and Fe; likely from precipitation/dissolution and redox changes, respectively; Figs. 2–4), these reactions appeared kinetically slow, limiting their impact on major geochemistry during the study period (Gillon et al., 2012).

This study also highlights the inadequacy of deploying grab-style sampling to capture transient shifts in fDOM parameters, particularly tryptophan-like fluorescence and FI. This is an important consideration for future studies, particularly as many have demonstrated that tryptophan detection can serve as method of bacterial metabolic activity, with the potential as a rapid *in-situ* microbial quality detection method in aqueous environments (Baker, 2002; Fox et al., 2017; Sorensen et al., 2016). Though, it is inherently difficult to disentangle confounding variables affecting DOM-related water quality in groundwater potentially affected by numerous (hydro)geological factors.

5. Conclusion

This study offers novel insight into the compositional changes to organic geochemistry in groundwater of West Bengal at the onset of monsoon. This study highlights large shifts in fDOM parameters, particularly tryptophan-like fluorescence and FI, over relatively short periods of time. Whilst total DOC remained fairly constant in groundwater, rainfall-associated fluctuations in FI alluded to an increase in metabolic activity and thus an activation of microbes following rainfall events. Geochemical indicators (*e.g.* *Eh* and FI) demonstrated that the

laterite-capped and pumped area around Kharagpur and Midnapore exhibited a more intermittent signal that was characteristic of macropore-dominated flow, which could be associated with cracking in laterites or ineffective borehole sealing, rather than aquifer-wide phenomena. Evidence from isotopes suggested that near-bank groundwater (*e.g.* at K2_15 and K3_18) was similar to local rivers, whilst some water (*e.g.* at K9_20 and K5_67) exhibited a signal typical of rapid surface-water ingression mixed with groundwater subject to evaporative enrichment. Major geochemistry was broadly consistent across the sampling timeframe, though a reduction in Ca could be a result of an increase to organic-derived alkalinity. Our findings provide novel insights into rainfall-DOM associations in aquifers in northern India and in similar geochemical settings. This research has application in water-stressed and/or groundwater-reliant regions of the world and advances knowledge in the field of groundwater quality monitoring.

CRediT authorship contribution statement

George J.L. Wilson: Writing – review & editing, Writing – original draft, Visualization, Validation, Methodology, Investigation, Formal analysis, Data curation, Conceptualization. **David A. Aind:** Writing – review & editing, Investigation, Formal analysis, Data curation. **Abhijit Mukherjee:** Writing – review & editing, Resources, Project administration. **David A. Polya:** Writing – review & editing, Supervision, Resources, Project administration, Methodology, Funding acquisition, Conceptualization. **Daren C. Gooddy:** Writing – review & editing, Supervision, Resources, Project administration, Methodology, Funding acquisition, Conceptualization. **Laura A. Richards:** Writing – review & editing, Supervision, Resources, Project administration, Methodology, Funding acquisition, Data curation, Conceptualization.

Declaration of competing interest

The authors declare that they have no known competing financial interests or personal relationships that could have appeared to influence the work reported in this paper.

Acknowledgements

Appendix A. Supplementary data

Supplementary data to this article can be found online at https://doi.

org/10.1016/j.apgeochem.2025.106298.

Data availability

Suitable data will be made available on reasonable request.

References

Aftabtalab, A., Rinklebe, J., Shaheen, S.M., Niazi, N.K., Moreno-Jiménez, E., Schaller, J., Knorr, K.-H.H., 2022. Review on the interactions of arsenic, iron (oxy)(hydr) oxides, and dissolved organic matter in soils, sediments, and groundwater in a ternary system. Chemosphere 286, 131790. https://doi.org/10.1016/j.chemosphere.2021.131790.

Baker, A., 2002. Fluorescence properties of some farm wastes: implications for water quality monitoring. Water Res. 36, 189–195. https://doi.org/10.1016/S0043-1354(01)00210-X.

Banks, E.W., Cook, P.G., Owor, M., Okullo, J., Kebede, S., Nedaw, D., Mleta, P., Fallas, H., Gooddy, D., John MacAllister, D., Mkandawire, T., Makuluni, P., Shaba, C.E., MacDonald, A.M., 2021. Environmental tracers to evaluate groundwater residence times and water quality risk in shallow unconfined aquifers in sub Saharan Africa. J. Hydrol. 598, 125753. https://doi.org/10.1016/j.jhydrol.2020.125753.

Benedetti, M.F., Riemsdijk, W.H.V., Koopal, L.K., Kinniburgh, D.G., Gooddy, D.C., Milne, C.J., 1996. Metal ion binding by natural organic matter: from the model to the field. Geochim. Cosmochim. Acta 60, 2503–2513.

Benner, S.G., Polizzotto, M.L., Kocar, B.D., Ganguly, S., Phan, K., Ouch, K., Sampson, M., Fendorf, S., 2008. Groundwater flow in an arsenic-contaminated aquifer, Mekong Delta, Cambodia. Appl. Geochem. 23, 3072–3087. https://doi.org/10.1016/j.apgeochem.2008.06.013.

Berthomieu, C., Hienerwadel, R., 2009. Fourier transform infrared (FTIR) spectroscopy. Photosynth. Res. 101, 157–170. https://doi.org/10.1007/s11120-009-9439-x.

Bhunia, P., Das, P., Maiti, R., 2020. Meteorological drought study through SPI in three drought prone districts of West Bengal, India. Earth Syst. Environ. 4, 43–55. https://doi.org/10.1007/s41748-019-00137-6.

Bianchi, T.S., 2011. The role of terrestrially derived organic carbon in the coastal ocean: a changing paradigm and the priming effect. Proc. Natl. Acad. Sci. U. S. A. 108, 19473–19481. https://doi.org/10.1073/pnas.1017982108.

Boyd, C.E., Tucker, C.S., Viriyatum, R., 2011. Interpretation of pH, acidity, and alkalinity in aquaculture and fisheries. North Am. J. Aquac. 73, 403–408. https://doi.org/10.1080/15222055.2011.620861.

Brailsford, F.L., Glanville, H.C., Marshall, M.R., Golyshin, P.N., Johnes, P.J., Yates, C.A., Owen, A.T., Jones, D.L., 2017. Microbial use of low molecular weight DOM in filtered and unfiltered groundwater: role of ultra-small microorganisms and implications for water quality monitoring. Sci. Total Environ. 598, 377–384. https://doi.org/10.1016/J.SCITOTENV.2017.04.049.

CGWB, 2023. Report on the dynamic ground water resources of West Bengal (No. 298). Technical Report Series D. Central Ground Water Board, Kolkata.

CGWB, 2022. Ground water yearbook of West Bengal & andaman & nicobar islands (2021-2022) (No. 287). Technical Report Series D. Central Ground Water Board, Kolkata.

Chatterjee, R., 2024. Spatiotemporal variation in physico-chemical properties of groundwater within arsenic-affected shallow alluvial aquifers of Murshidabad district, West Bengal, eastern India. In: Ground Water Contamination in India: Adverse Effects on Habitats. Springer, pp. 33–82.

Chen, S., Zhong, J., Ran, L., Yi, Y., Wang, W., Yan, Z., Li, S., Mostofa, K.M.G., 2022. Geographical controls and anthropogenic impacts on dissolved organic carbon from mountainous rivers: insights from optical properties and carbon isotopes. https://doi.org/10.5194/bg-2022-217.

Chen, X., Liu, M., Kuzyakov, Y., Li, W., Liu, J., Jiang, C., Wu, M., Li, Z., 2018. Incorporation of rice straw carbon into dissolved organic matter and microbial biomass along a 100-year paddy soil chronosequence. Appl. Soil Ecol. 130, 84–90. https://doi.org/10.1016/J.APSOIL.2018.06.004.

Chowdhury, A., Jha, M.K., Chowdary, V.M., 2010. Delineation of groundwater recharge zones and identification of artificial recharge sites in West Medinipur district, West Bengal, using RS, GIS and MCDM techniques. Environ. Earth Sci. 59, 1209–1222. https://doi.org/10.1007/S12665-009-0110-9/FIGURES/11.

Cory, R.M., McKnight, D.M., 2005. Fluorescence spectroscopy reveals ubiquitous presence of oxidized and reduced quinones in dissolved organic matter. Environ. Sci. Technol. 39, 8142–8149. https://doi.org/10.1021/es0506962.

Craig, H., 1961. Isotopic variations in meteoric waters. Science 133, 1702–1703.

Dangar, S., Asoka, A., Mishra, V., 2021. Causes and implications of groundwater depletion in India: a review. J. Hydrol. 596, 126103. https://doi.org/10.1016/j.jhydrol.2021.126103.

Datta, S., Neal, A.W., Mohajerin, T.J., Ocheltree, T., Rosenheim, B.E., White, C.D., Johannesson, K.H., 2011. Perennial ponds are not an important source of water or dissolved organic matter to groundwaters with high arsenic concentrations in West Bengal, India. Geophys. Res. Lett. 38. https://doi.org/10.1029/2011GL049301 n/a-n/a.

Dittmar, T., Paeng, J., 2009. A heat-induced molecular signature in marine dissolved organic matter. Nat. Geosci. 2, 175–179. https://doi.org/10.1038/ngeo440.

Ercumen, A., Naser, A.M., Arnold, B.F., Unicomb, L., Colford Jr, J.M., Luby, S.P., 2017. Can sanitary inspection surveys predict risk of microbiological contamination of groundwater sources? Evidence from shallow tubewells in rural Bangladesh. Am. J. Trop. Med. Hyg. 96, 561.

Evans, S., Campbell, C., Naidenko, O.V., 2019. Cumulative risk analysis of carcinogenic contaminants in United States drinking water. Heliyon 5.

Fang, Q., Lu, A., Hong, H., Kuzyakov, Y., Algeo, T.J., Zhao, L., Olshansky, Y., Moravec, B., Barrientes, D.M., Chorover, J., 2023. Mineral weathering is linked to microbial priming in the critical zone. Nat. Commun. 14, 345. https://doi.org/10.1038/s41467-022-35671-x.

Farooq, S.H., Chandrasekharam, D., Berner, Z., Norra, S., Stüben, D., 2010. Influence of traditional agricultural practices on mobilization of arsenic from sediments to groundwater in Bengal delta. Water Res. 44, 5575–5588. https://doi.org/10.1016/j.watres.2010.05.057.

Farooq, S.H., Chandrasekharam, D., Norra, S., Berner, Z., Eiche, E., Thambidurai, P., Stüben, D., 2011. Temporal variations in arsenic concentration in the groundwater of Murshidabad District, West Bengal, India. Environ. Earth Sci. 62, 223–232. https://doi.org/10.1007/s12665-010-0516-4.

Fontaine, S., Barot, S., Barré, P., Bdioui, N., Mary, B., Rumpel, C., 2007. Stability of organic carbon in deep soil layers controlled by fresh carbon supply. Nature 450, 277–280. https://doi.org/10.1038/nature06275.

Fox, B.G., Thorn, R.M.S., Anesio, A.M., Reynolds, D.M., 2017. The in situ bacterial production of fluorescent organic matter; an investigation at a species level. Water Res. 125, 350–359. https://doi.org/10.1016/j.watres.2017.08.040.

Ghosh, S., Guchhait, S.K., Hu, X.-F., 2015. Characterization and evolution of primary and secondary laterites in northwestern Bengal Basin, West Bengal, India. J. Palaeogeogr. 4, 203–230. https://doi.org/10.3724/SP.J.1261.2015.00074.

Gillon, M., Renard, F., Crançon, P., Aupiais, J., 2012. Kinetics of incongruent dissolution of carbonates in a Chalk aquifer using reverse flow modelling. J. Hydrol. 420–421, 329–339. https://doi.org/10.1016/j.jhydrol.2011.12.025.

Gonfiantini, R., 1978. Standards for stable isotope measurements in natural compounds. Nature 271, 534–536.

Graham, P.W., Baker, A., Andersen, M.S., 2015. Dissolved organic carbon mobilisation in a groundwater system stressed by pumping. Sci. Rep. 5, 18487. https://doi.org/10.1038/srep18487.

Groeneveld, M., Catalán, N., Attermeyer, K., Hawkes, J., Einarsdóttir, K., Kothawala, D., Bergquist, J., Tranvik, L., 2020. Selective adsorption of terrestrial dissolved organic matter to inorganic surfaces along a boreal inland water continuum. J. Geophys. Res. Biogeosciences 125, e2019JG005236. https://doi.org/10.1029/2019JG005236.

Hofmann, R., Uhl, J., Hertkorn, N., Griebler, C., 2020. Linkage between dissolved organic matter transformation, bacterial carbon production, and diversity in a shallow oligotrophic aquifer: results from flow-through sediment microcosm experiments. Front. Microbiol. 11. https://doi.org/10.3389/fmicb.2020.543567.

Howard, G., Pedley, S., Barrett, M., Nalubega, M., Johal, K., 2003. Risk factors contributing to microbiological contamination of shallow groundwater in Kampala, Uganda. Water Res. 37, 3421–3429. https://doi.org/10.1016/S0043-1354(03)00235-5.

Hynds, P.D., Misstear, B.D., Gill, L.W., 2012. Development of a microbial contamination susceptibility model for private domestic groundwater sources. Water Resour. Res. 48, 1–13. https://doi.org/10.1029/2012WR012492.

IAEA/WMO, 2017. Water Isotope System for Data Analysis, Visualization and Electronic Retrieval (WISER).

Islam, F.S., Gault, A.G., Boothman, C., Polya, D.A., Chamok, J.M., Chatterjee, D., Lloyd, J.R., Charnock, J.M., Chatterjee, D., Lloyd, J.R., 2004. Role of Metal-Reducing Bacteria in Arsenic Release from Bengal Delta Sediments, Nature. Nature Publishing Group. https://doi.org/10.1038/nature02638.

Jain, M., Fishman, R., Mondal, P., Galford, G.L., Bhattarai, N., Naeem, S., Lall, U., Balwinder-Singh, DeFries, R.S., 2021. Groundwater depletion will reduce cropping intensity in India. Sci. Adv. 7. https://doi.org/10.1126/sciadv.abd2849.

Jameel, Y., Stahl, M., Michael, H., Bostick, B.C., Steckler, M.S., Schlosser, P., Van Geen, A., Harvey, C., 2023. Shift in groundwater recharge of the Bengal Basin from rainfall to surface water. Commun. Earth Environ. 4, 14. https://doi.org/10.1038/s43247-022-00650-z.

Jana, S., Pahari, P.R., Dutta, T.K., Bhattacharya, T., 2009. Diversity and community structure of aquatic insects in a pond in Midnapore town, West Bengal, India. J. Environ. Biol. 30, 283–287.

Jiang, C., Garg, S., Waite, T.D., 2015. Hydroquinone-mediated redox cycling of iron and concomitant oxidation of hydroquinone in oxic waters under acidic conditions: comparison with iron–natural organic matter interactions. Environ. Sci. Technol. 49, 14076–14084. https://doi.org/10.1021/acs.est.5b03189.

John, B., Das, R., Das, S., 2018. An overview of the development of groundwater resources in India with special reference to West Bengal and Kolkata. Int. J. Emerg. Trends Eng. Dev. 3. https://doi.org/10.26808/rs.ed.i8v3.01.

Kerr, D.E., Brown, P.J., Grey, A., Kelleher, B.P., 2021. The influence of organic alkalinity on the carbonate system in coastal waters. Mar. Chem. 237, 104050. https://doi.org/10.1016/j.marchem.2021.104050.

Kim, H., Lee, K., 2009. Significant contribution of dissolved organic matter to seawater alkalinity. Geophys. Res. Lett. 36, 2009GL040271. https://doi.org/10.1029/2009GL040271.

Klose, T., Chaparro, M.C., Schilling, F., Butscher, C., Klumbach, S., Blum, P., 2021. Fluid flow simulations of a large-scale borehole leakage experiment. Transp. Porous Media 136, 125–145. https://doi.org/10.1007/s11242-020-01504-y.

Kulkarni, H.V., Mladenov, N., Datta, S., Chatterjee, D., 2018. Influence of monsoonal recharge on arsenic and dissolved organic matter in the Holocene and Pleistocene aquifers of the Bengal Basin. Sci. Total Environ. 637–638, 588–599. https://doi.org/10.1016/j.scitotenv.2018.05.009.

Kulkarni, H.V., Mladenov, N., Johannesson, K.H., Datta, S., 2017. Contrasting dissolved organic matter quality in groundwater in Holocene and Pleistocene aquifers and implications for influencing arsenic mobility. Appl. Geochem. 77, 194–205. https://doi.org/10.1016/j.apgeochem.2016.06.002.

Kuzyakov, Y., 2010. Priming effects: interactions between living and dead organic matter. Soil Biol. Biochem. 42, 1363–1371. https://doi.org/10.1016/j.soilbio.2010.04.003.

Kwak, K., Varner, T.S., Nguyen, W., Kulkarni, H.V., Buskirk, R., Huang, Y., Saeed, A., Hosain, A., Aitkenhead-Peterson, J., Ahmed, K.M., Akhter, S.H., Cardenas, M.B., Datta, S., Knappett, P.S.K., 2024. Hotspots of dissolved arsenic generated from buried silt layers along fluctuating rivers. Environ. Sci. Technol. https://doi.org/10.1021/acs.est.4c02330.

Lakowicz, J.R., 1994. Topics in Fluorescence Spectroscopy: Volume 4: Probe Design and Chemical Sensing. Springer Science & Business Media.

Lapworth, D.J., Boving, T.B., Kreamer, D.K., Kebede, S., Smedley, P.L., 2022. Groundwater quality: global threats, opportunities and realising the potential of groundwater. Sci. Total Environ. 811, 152471. https://doi.org/10.1016/j.scitotenv.2021.152471.

Lapworth, D.J., Kinniburgh, D.G., 2009. An R script for visualising and analysing fluorescence excitation–emission matrices (EEMs). Comput. Geosci. 35, 2160–2163. https://doi.org/10.1016/j.cageo.2008.10.013.

Lawson, M., Polya, D.A., Boyce, A.J., Bryant, C., Ballentine, C.J., 2016. Tracing organic matter composition and distribution and its role on arsenic release in shallow Cambodian groundwaters. Geochim. Cosmochim. Acta 178, 160–177. https://doi.org/10.1016/j.gca.2016.01.010.

Leenheer, J.A., Croué, J.-P., 2003. Characterizing aquatic dissolved organic matter. Environmental science and Technology. UTC.

Li, M., He, Y.-S., Kang, J.-T., Yang, X.-Y., He, Z.-W., Yu, H.-M., Huang, F., 2017. Why was iron lost without significant isotope fractionation during the lateritic process in tropical environments? Geoderma 290, 1–9. https://doi.org/10.1016/j.geoderma.2016.12.003.

Liu, D., She, D., 2020. The effect of fracture properties on preferential flow in carbonate-derived laterite from karst mountainous agroforestry lands. Soil Tillage Res. 203, 104670. https://doi.org/10.1016/j.still.2020.104670.

Lu, C., Richards, L.A., Wilson, G.J.L., Krause, S., Lapworth, D.J., Gooddy, D.C., Chakravorty, B., Polya, D.A., Niasar, V.J., 2022. Quantifying the impacts of groundwater abstraction on Ganges river water infiltration into shallow aquifers under the rapidly developing city of Patna, India. J. Hydrol. Reg. Stud. 42, 101133. https://doi.org/10.1016/J.EJRH.2022.101133.

Luzius, C., Guillemette, F., Podgorski, D.C., Kellerman, A.M., Spencer, R.G.M., 2018. Drivers of dissolved organic matter in the vent and major conduits of the world's largest freshwater spring. J. Geophys. Res. Biogeosciences 123, 2775–2790. https://doi.org/10.1029/2017JG004327.

Majumder, S., Datta, S., Nath, B., Neidhardt, H., Sarkar, S., Roman-Ross, G., Berner, Z., Hidalgo, M., Chatterjee, Debankur, Chatterjee, Debashis, 2016. Monsoonal influence on variation of hydrochemistry and isotopic signatures: implications for associated arsenic release in groundwater. J. Hydrol. 535, 407–417. https://doi.org/10.1016/j.jhydrol.2016.01.052.

Matilainen, A., Gjessing, E.T., Lahtinen, T., Hed, L., Bhatnagar, A., Sillanpää, M., 2011. An overview of the methods used in the characterisation of natural organic matter (NOM) in relation to drinking water treatment. Chemosphere 83, 1431–1442. https://doi.org/10.1016/J.CHEMOSPHERE.2011.01.018.

McArthur, J.M., Banerjee, D.M., Sengupta, S., Ravenscroft, P., Klump, S., Sarkar, A., Disch, B., Kipfer, R., 2010. Migration of As, and 3H/3He ages, in groundwater from West Bengal: implications for monitoring. Water Res. 44, 4171–4185. https://doi.org/10.1016/j.watres.2010.05.010.

McDonough, L.K., Santos, I.R., Andersen, M.S., O'Carroll, D.M., Rutlidge, H., Meredith, K., Oudone, P., Bridgeman, J., Gooddy, D.C., Sorensen, J.P.R., Lapworth, D.J., MacDonald, A.M., Ward, J., Baker, A., 2020. Changes in global groundwater organic carbon driven by climate change and urbanization. Nat. Commun. 11, 1–10. https://doi.org/10.1038/s41467-020-14946-1.

McKnight, D.M., Boyer, E.W., Westerhoff, P.K., Doran, P.T., Kulbe, T., Andersen, D.T., 2001. Spectrofluorometric characterization of dissolved organic matter for indication of precursor organic material and aromaticity. Limnol. Oceanogr. 46, 38–48. https://doi.org/10.4319/lo.2001.46.1.0038.

Miller, J.N., Miller, J.C., 2010. Statistics and Chemometrics for Analytical Chemistry, sixth ed. Prentice Hall/Pearson, Harlow.

Mladenov, N., Zheng, Y., Miller, M.P., Nemergut, D.R., Legg, T., Simone, B., Hageman, C., Rahman, M.M., Ahmed, K.M., Mcknight, D.M., 2010. Dissolved organic matter sources and consequences for iron and arsenic mobilization in Bangladesh aquifers. Environ. Sci. Technol. 44, 123–128. https://doi.org/10.1021/es901472g.

Mohanta, T., Goel, S., 2014. Assessment of water quality of three different aquatic environments over three seasons. In: 1st International Congress on Environmental, Biotechnology, and Chemistry Engineering. https://doi.org/10.7763/IPCBEE.

Mukherjee, A. (Ed.), 2022. Riverine Systems: Understanding the Hydrological, Hydrosocial and Hydro-Heritage Dynamics. Springer International Publishing, Cham. https://doi.org/10.1007/978-3-030-87067-6.

Murphy, K.R., 2011. A note on determining the extent of the water Raman peak in fluorescence spectroscopy. Appl. Spectrosc. 65, 233–236.

Murphy, K.R., Stedmon, C.A., Graeber, D., Bro, R., 2013. Fluorescence spectroscopy and multi-way techniques. PARAFAC. Anal. Methods 5, 6557–6566. https://doi.org/10.1039/c3ay41160e.

Neidhardt, H., Biswas, A., Freikowski, D., Majumder, S., Chatterjee, D., Berner, Z.A., 2013. Reconstructing the sedimentation history of the Bengal Delta Plain by means of geochemical and stable isotopic data. Appl. Geochem. 36, 70–82. https://doi.org/10.1016/j.apgeochem.2013.06.017.

Niloy, N.M., Haque, M.M., Tareq, S.M., 2021. Characteristics, sources, and seasonal variability of dissolved organic matter (DOM) in the ganges river, Bangladesh. Environ. Process. 8, 593–613.

Ohno, T., 2002. Fluorescence inner-filtering correction for determining the humification index of dissolved organic matter. Environ. Sci. Technol. 36, 742–746. https://doi.org/10.1021/es0155276.

Osburn, C.L., Anderson, N.J., Stedmon, C.A., Giles, M.E., Whiteford, E.J., McGenity, T.J., Dumbrell, A.J., Underwood, G.J.C., 2017. Shifts in the source and composition of dissolved organic matter in southwest Greenland lakes along a regional hydro-climatic gradient. J. Geophys. Res. Biogeosciences 122, 3431–3445. https://doi.org/10.1002/2017JG003999.

Pagano, T., Bida, M., Kenny, J., 2014. Trends in levels of allochthonous dissolved organic carbon in natural water: a review of potential mechanisms under a changing climate. Water 6, 2862–2897. https://doi.org/10.3390/w6102862.

Pai, D.S., Rajeevan, M., Sreejith, O.P., Mukhopadhyay, B., Satbha, N.S., 2014. Development of a new high spatial resolution (0.25° × 0.25°) long period (1901-2010) daily gridded rainfall data set over India and its comparison with existing data sets over the region. Mausam 65, 1–18. https://doi.org/10.54302/mausam.v65i1.851.

Panda, K.P., Sharma, S.P., Jha, M.K., 2018. Mapping lithological variations in a river basin of West Bengal, India using electrical resistivity survey: implications for artificial recharge. Environ. Earth Sci. 77, 1–10. https://doi.org/10.1007/S12665-018-7813-8/FIGURES/7.

Parlanti, E., Wörz, K., Geoffroy, L., Lamotte, M., 2000. Dissolved organic matter fluorescence spectroscopy as a tool to estimate biological activity in a coastal zone submitted to anthropogenic inputs. Org. Geochem. 31, 1765–1781. https://doi.org/10.1016/S0146-6380(00)00124-8.

Piper, A.M., 1944. A graphic procedure in the geochemical interpretation of water-analyses. Eos Trans. Am. Geophys. Union 25, 914–928. https://doi.org/10.1029/TR025i006p00914.

Postma, D., Larsen, F., Minh Hue, N.T., Duc, M.T., Viet, P.H., Nhan, P.Q., Jessen, S., 2007. Arsenic in groundwater of the Red River floodplain, Vietnam: controlling geochemical processes and reactive transport modeling. Geochim. Cosmochim. Acta 71, 5054–5071. https://doi.org/10.1016/j.gca.2007.08.020.

Pracný, P., Faimon, J., Všianský, D., Přichystal, A., 2019. Evolution of Mg/Ca and Sr/Ca ratios during the experimental dissolution of limestone. Chem. Geol. 523, 107–120. https://doi.org/10.1016/j.chemgeo.2019.05.040.

Qualls, R.G., Richardson, C.J., 2003. Factors controlling concentration, export, and decomposition of dissolved organic nutrients in the Everglades of Florida. Biogeochemistry 62, 197–229.

R Core Team, 2023. R: A Language and Environment for Statistical Computing.

Ren, Z.-L., Tella, M., Bravin, M.N., Comans, R.N.J., Dai, J., Garnier, J.-M., Sivry, Y., Doelsch, E., Straathof, A., Benedetti, M.F., 2015. Effect of dissolved organic matter composition on metal speciation in soil solutions. Chem. Geol. 398, 61–69. https://doi.org/10.1016/j.chemgeo.2015.01.020.

Richards, L.A., Lapworth, D.J., Magnone, D., Gooddy, D.C., Chambers, L., Williams, P.J., van Dongen, B.E., Polya, D.A., 2019a. Dissolved organic matter tracers reveal contrasting characteristics across high arsenic aquifers in Cambodia: a fluorescence spectroscopy study. Geosci. Front. 10, 1653–1667. https://doi.org/10.1016/j.gsf.2019.04.009.

Richards, L.A., Magnone, D., Sovann, C., Kong, C., Uhlemann, S., Kuras, O., van Dongen, B.E., Ballentine, C.J., Polya, D.A., 2017. High resolution profile of inorganic aqueous geochemistry and key redox zones in an arsenic bearing aquifer in Cambodia. Sci. Total Environ. 590–591, 540–553. https://doi.org/10.1016/j.scitotenv.2017.02.217.

Richards, L.A., Magnone, D., Sültenfuß, J., Chambers, L., Bryant, C., Boyce, A.J., Van Dongen, B.E., Ballentine, C.J., Sovann, C., Uhlemann, S., Kuras, O., Gooddy, D.C., Polya, D.A., 2019b. Dual in-aquifer and near surface processes drive arsenic mobilization in Cambodian groundwaters. Sci. Total Environ. 659, 699–714. https://doi.org/10.1016/j.scitotenv.2018.12.437.

Rodell, M., Velicogna, I., Famiglietti, J.S., 2009. Satellite-based estimates of groundwater depletion in India. Nature 460, 999–1002. https://doi.org/10.1038/nature08238.

Rowland, H.A.L., Pederick, R.L., Polya, D.A., Pancost, R.D., Van Dongen, B.E., Gault, A. G., Vaughan, D.J., Bryant, C., Anderson, B., Lloyd, J.R., 2007. The control of organic matter on microbially mediated iron reduction and arsenic release in shallow alluvial aquifers, Cambodia. Geobiology 5, 281–292. https://doi.org/10.1111/j.1472-4669.2007.00100.x.

Roy, S., Soren, R., Hazra, S., 2023. Benefits of reviving indigenous water conservation practices for drought resilience in red and lateritic zones of West Bengal, India. In: Indigenous and Local Water Knowledge, Values and Practices. Springer, pp. 175–197.

Sarkar, H., Ray, S.P.S., 2015. Large scale of water supply Scheme in recent alluvium water table aquifer on the river bed and palleo-channel deposit of the river Subarnarekha in Nayagram block, West Midnapore district, West Bengal. J. Cent. Ground Water Stud. 4, 67–84.

Schaefer, M.V., Ying, S.C., Benner, S.G., Duan, Y., Wang, Y., Fendorf, S., 2016. Aquifer arsenic cycling induced by seasonal hydrologic changes within the yangtze river basin. Environ. Sci. Technol. 50, 3521–3529. https://doi.org/10.1021/acs.est.5b04986.

Schmidt, M.W.I., Torn, M.S., Abiven, S., Dittmar, T., Guggenberger, G., Janssens, I.A., Kleber, M., Kögel-Knabner, I., Lehmann, J., Manning, D.A.C., 2011. Persistence of soil organic matter as an ecosystem property. Nature 478, 49–56.

Sgroi, M., Roccaro, P., Korshin, G.V., Vagliasindi, F.G.A., 2017. Monitoring the behavior of emerging contaminants in wastewater-impacted rivers based on the use of fluorescence excitation emission matrixes (EEM). Environ. Sci. Technol. 51, 4306–4316. https://doi.org/10.1021/acs.est.6b05785.

Sinclair, D.J., Banner, J.L., Taylor, F.W., Partin, J., Jenson, J., Mylroie, J., Goddard, E., Quinn, T., Jocson, J., Miklavič, B., 2012. Magnesium and strontium systematics in

tropical speleothems from the Western Pacific. Chem. Geol. 294–295, 1–17. https://doi.org/10.1016/j.chemgeo.2011.10.008.

Singh, A., Patel, A.K., Deka, J.P., Das, A., Kumar, A., Kumar, M., 2020. Prediction of arsenic vulnerable zones in the groundwater environment of a rapidly urbanizing setup, Guwahati, India. Geochemistry 80, 125590. https://doi.org/10.1016/j.chemer.2019.125590.

Singh, L.P., Parkash, B., Singhvi, A.K., 1998. Evolution of the lower gangetic plain landforms and soils in West Bengal, India. Catena 33, 75–104. https://doi.org/10.1016/S0341-8162(98)00066-6.

Sorensen, J.P.R., Baker, A., Cumberland, S.A., Lapworth, D.J., MacDonald, A.M., Pedley, S., Taylor, R.G., Ward, J.S.T., 2018a. Real-time detection of faecally contaminated drinking water with tryptophan-like fluorescence: defining threshold values. Sci. Total Environ. 622–623, 1250–1257. https://doi.org/10.1016/j.scitotenv.2017.11.162.

Sorensen, J.P.R., Diaw, M.T., Pouye, A., Roffo, R., Diongue, D.M.L., Faye, S.C., Gaye, C.B., Fox, B.G., Goodall, T., Lapworth, D.J., MacDonald, A.M., Read, D.S., Ciric, L., Taylor, R.G., 2020. In-situ fluorescence spectroscopy indicates total bacterial abundance and dissolved organic carbon. Sci. Total Environ. 738, 139419. https://doi.org/10.1016/J.SCITOTENV.2020.139419.

Sorensen, J.P.R., Nayebare, J., Carr, A.F., Lyness, R., Campos, L.C., Ciric, L., Goodall, T., Kulabako, R., Curran, C.M.R., MacDonald, A.M., Owor, M., Read, D.S., Taylor, R.G., 2021. In-situ fluorescence spectroscopy is a more rapid and resilient indicator of faecal contamination risk in drinking water than faecal indicator organisms. Water Res. 206, 117734. https://doi.org/10.1016/j.watres.2021.117734.

Sorensen, J.P.R., Sadhu, A., Sampath, G., Sugden, S., Dutta Gupta, S., Lapworth, D.J., Marchant, B.P., Pedley, S., 2016. Are sanitation interventions a threat to drinking water supplies in rural India? An application of tryptophan-like fluorescence. Water Res. 88, 923–932. https://doi.org/10.1016/j.watres.2015.11.006.

Sorensen, J.P.R., Vivanco, A., Ascott, M.J., Gooddy, D.C., Lapworth, D.J., Read, D.S., Rushworth, C.M., Bucknall, J., Herbert, K., Karapanos, I., Gumm, L.P., Taylor, R.G., 2018b. Online fluorescence spectroscopy for the real-time evaluation of the microbial quality of drinking water. Water Res. 137, 301–309. https://doi.org/10.1016/j.watres.2018.03.001.

Stedmon, C.A., Markager, S., 2005. Resolving the variability in dissolved organic matter fluorescence in a temperate estuary and its catchment using PARAFAC analysis. Limnol. Oceanogr. 50, 686–697. https://doi.org/10.4319/LO.2005.50.2.0686.

Sulpis, O., Agrawal, P., Wolthers, M., Munhoven, G., Walker, M., Middelburg, J.J., 2022. Aragonite dissolution protects calcite at the seafloor. Nat. Commun. 13, 1104. https://doi.org/10.1038/s41467-022-28711-z.

Takavada, I., Hoko, Z., Gumindoga, W., Mhizha, A., Nuttinck, J.Y., Faure, G., Malik, D., 2022. An assessment on the effectiveness of the sanitary seal in protecting boreholes from contamination: a case of Mbare Suburb, Harare. Phys. Chem. Earth 126, 103107. https://doi.org/10.1016/j.pce.2022.103107.

Uhlemann, S., Kuras, O., Richards, L.A., Naden, E., Polya, D.A., 2017. Electrical resistivity tomography determines the spatial distribution of clay layer thickness and aquifer vulnerability, Kandal Province, Cambodia. J. Asian Earth Sci. 147, 402–414. https://doi.org/10.1016/j.jseaes.2017.07.043.

Wallis, I., Prommer, H., Berg, M., Siade, A.J., Sun, J., Kipfer, R., 2020. The river–groundwater interface as a hotspot for arsenic release. Nat. Geosci. 13, 288–295. https://doi.org/10.1038/s41561-020-0557-6.

Ward, J.S.T., Lapworth, D.J., Read, D.S., Pedley, S., Banda, S.T., Monjerezi, M., Gwengweya, G., Macdonald, A.M., 2021. Tryptophan-like fluorescence as a high-level screening tool for detecting microbial contamination in drinking water. Sci. Total Environ. 750, 141284. https://doi.org/10.1016/j.scitotenv.2020.141284.

Weishaar, J.L., Aiken, G.R., Bergamaschi, B.A., Fram, M.S., Fujii, R., Mopper, K., 2003. Evaluation of specific ultraviolet absorbance as an indicator of the chemical composition and reactivity of dissolved organic carbon. Environ. Sci. Technol. 37, 4702–4708. https://doi.org/10.1021/es030360x.

Wilson, G.J.L., Lu, C., Lapworth, D.J., Kumar, A., Ghosh, A., Niasar, V.J., Krause, S., Polya, D.A., Gooddy, D.C., Richards, L.A., 2023. Spatial and seasonal controls on dissolved organic matter composition in shallow aquifers under the rapidly developing City of Patna, India. Sci. Total Environ. 166208.

Worrall, F., Burt, T., 2004. Time series analysis of long-term river dissolved organic carbon records. Hydrol. Process. 18, 893–911. https://doi.org/10.1002/hyp.1321.

Worrall, F., Burt, T.P., 2007. Flux of dissolved organic carbon from U.K. rivers. Glob. Biogeochem. Cycles 21, 2006GB002709. https://doi.org/10.1029/2006GB002709.

Worthington, S.R.H., Smart, C.C., 2017. Contamination bactérienne transitoire d'un aquifère à double-porosité à Walkerton, Ontario, Canada. Hydrogeol. J. 25, 1003–1016. https://doi.org/10.1007/s10040-016-1514-8.

Wünsch, U., Bro, R., Stedmon, C., Wenig, P., Murphy, K., 2019. Emerging patterns in the global distribution of dissolved organic matter fluorescence. Anal. Methods 11, 888–893. https://doi.org/10.1039/C8AY02422G.

Yamashita, Y., Kloeppel, B.D., Knoepp, J., Zausen, G.L., Jaffé, R., 2011. Effects of watershed history on dissolved organic matter characteristics in headwater streams. Ecosystems 14, 1110–1122. https://doi.org/10.1007/s10021-011-9469-z.

Yang, Y., Yuan, X., Deng, Y., Xie, X., Gan, Y., Wang, Y., 2020. Seasonal dynamics of dissolved organic matter in high arsenic shallow groundwater systems. J. Hydrol. 589, 125120. https://doi.org/10.1016/j.jhydrol.2020.125120.